DOE-PC-90054

Novel Nanodispersed Coal Liquefaction Catalysts: Molecular Design Via Microemulsion-Based Synthesis

Technical Progress Report
July - September 1993

by

E. Boakye, M. Vittal, K. Osseo-Asare and L. R. Radovic

Department of Materials Science and Engineering
The Pennsylvania State University
University Park, PA 16802

Prepared for the
United States Department of Energy
under
Contract No. DE-AC22-90PC90054

October 1993

Novel Nanodispersed Coal Liquefaction Catalysts: Molecular Design Via Microemulsion-Based Synthesis

Technical Progress Report

July - September 1993

by

E. Boakye, M. Vittal, K. Osseo-Asare and L. R. Radovic

Department of Materials Science and Engineering
The Pennsylvania State University
University Park, PA 16802

October 1993

DISCLAIMER

TABLE OF CONTENTS

PROJECT OBJECTIVES

The objective of this project is to pursue the development of highly dispersed and inexpensive catalysts for improved coal solubilization and upgrading of coal liquids. A novel study of the synthesis of liquefaction catalysts of nanometer size is being carried out. It is based on the molecular design of inverse micelles (microemulsions). These surfactant-stabilized, metal-bearing microdrops offer unique opportunities for synthesizing very small particles by providing a cage-like effect that limits particle nucleation, growth and agglomeration. The emphasis is on molybdenum- and iron-based catalysts, but the techniques being developed should also be generally applicable. The size of these very small and monodispersed particles will be accurately determined both separately and after *in situ* and *ex situ* coal impregnation. The as-prepared nanoparticles as well as the catalyst-impregnated coal matrix are characterized using a battery of techniques, including dynamic light scattering, x-ray diffraction and transmission electron microscopy. Catalytic activity tests are conducted under standardized coal liquefaction conditions. The effects of particle size of these unsupported catalysts on the product yield and distribution during conversion of a bituminous and a subbituminous coal are being determined.

TASK 1: CATALYST PREPARATION

Experimental

Figure 1 is a schematic illustration of the two synthesis protocols that were used in this study, namely (a) microemulsion plus a second reactant and (b) two microemulsions. There have been some reports in the literature that particles of different sizes are obtained when different synthesis protocols are used. For example, Lianos and Thomas (1987) reported results on the synthesis of CdS in the AOT/heptane/water microemulsion system. Particles of different sizes were obtained by using the microemulsion-plus-a-second-reactant and the two-microemulsions synthesis methods. The differences in particle size were attributed to unequal solubilization rates of the ions in the microemulsion system depending on the synthesis method. To make particles of predetermined size with greater certainty, we must know how factors such as (a) synthesis protocol, (b) water-to-surfactant molar ratio, and (c) the number of reactant species per inverse micelle (occupancy number) affect the particle size and size distribution.

Phase Behavior. The methodology of characterization of the phase behavior of the microemulsion system 0.15 M NP-5/cyclohexane/aqueous phase was the same as described in our previous reports. To check for the effect of the reactant species on the solubilization and solubility limits, the phase behavior of a number of samples containing 1.3×10^{-3} M sulfuric acid or 6.4×10^{-6} M ammonium tetrathiomolybdate and different water contents was observed as a function of temperature. The phase behavior of microemulsion samples containing only water was also recorded to check the effect of the electrolytes on the solubilization and the solubility limits. The measurements were reproducible within $\pm$ 0.5 °C for a given R value.

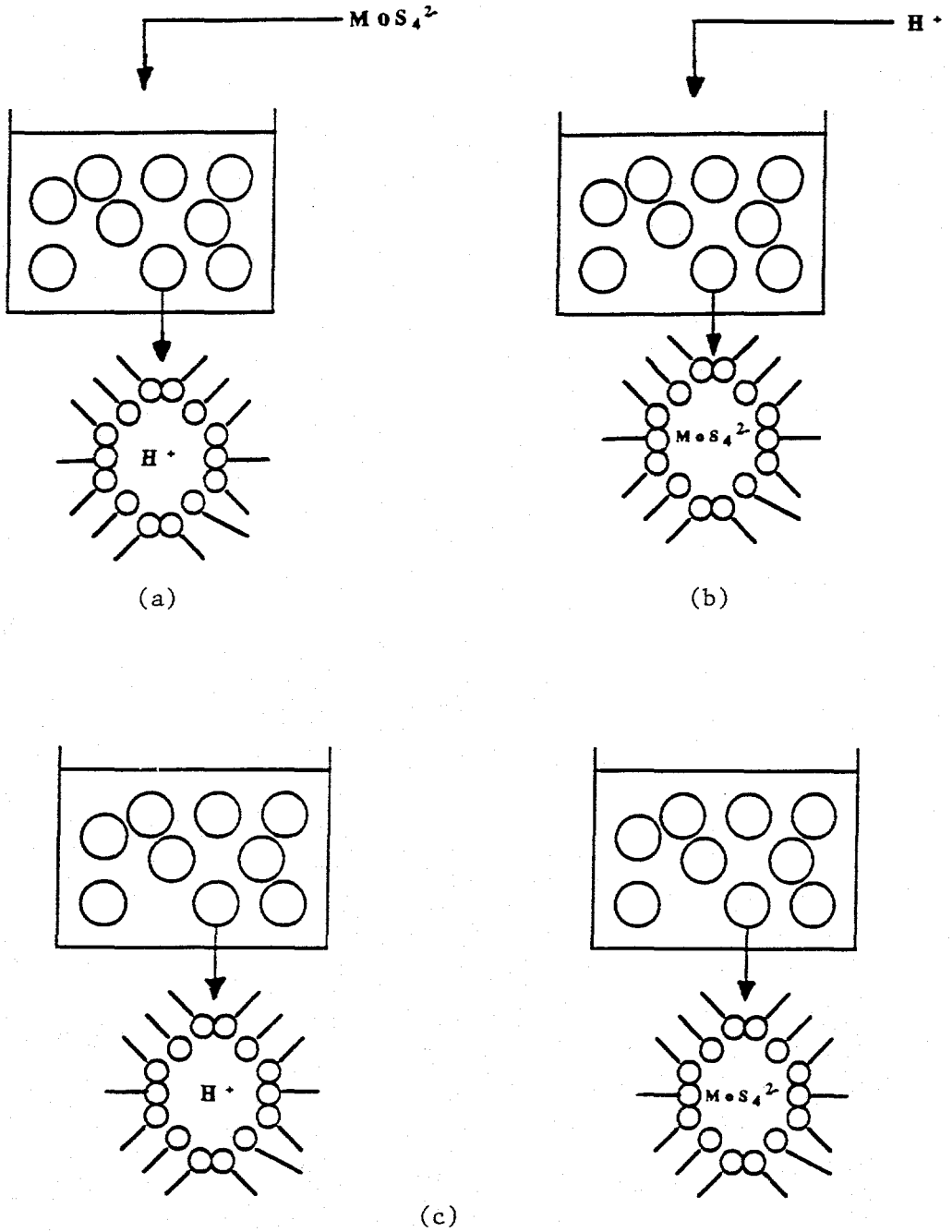

Figure 1. Particle synthesis methods in water-in-oil (w/o) microemulsions:
(a) thiomolybdate plus acid solubilized in microemulsion;
(b) acid plus thiomolybdate solubilized in microemulsions;
(c) two microemulsions.

Micellar Size Measurements. Photon correlation spectroscopy (PCS) was used to measure the microemulsion droplet size. The light source of the apparatus was a coherent Innova 70-2 argon ion laser operating at 488 nm. The scattered light was collected at an angle of 90° by a goniometer and focused on a photomultiplier tube (both from Malvern Instruments, Inc.). The correlation function was recorded with a Malvern 7032-8 correlator with 256 channels. The hydrodynamic size was calculated with a particle size distribution software also obtained from Malvern. Before micellar size measurements, the sample was centrifuged to remove dust and any particles that may exist in the microemulsion. The refractive index of cyclohexane was measured with an Abbe-3L refractometer (Milton Roy Company). The viscosity was determined with a Unbbelode viscometer immersed in a thermostated bath.

In the PCS technique the fluctuation in scattered intensity due to Brownian motion of the inverse micelles, which is represented by the intensity autocorrelation function, is measured over small time intervals. The magnitudes of a signal and its delayed version are compared. The measured intensity autocorrelation function $G(\tau)$ is related to the autocorrelation function $g(\tau)$ by the Equation 1.

$$G(\tau) = A(1 + B|g(\tau)|^2) \qquad (1)$$

(A and B are instrumental constants.) For polydispersed systems $g(\tau)$ deviates from a single exponential (i.e., one particle size representation). Hence the method of cumulants was used to analyze the data.

Particle Synthesis. For the microemulsion-plus-a-second-reactant method the following synthesis schemes were used (see Figures 1a and 1b). In scheme 1a, 12 μL of 1.1 M aqueous sulfuric acid was first solubilized in NP-5/cyclohexane while

bubbling high purity nitrogen gas. This was followed by adding 13 μL of $5x10^{-3}$ M ammonium tetrathiomolybdate. Nitrogen was further bubbled while molybdenum sulfide formed. On the other hand, for scheme 1b 13 μL of ammonium tetrathiomolybdate was first solubilized followed by addition of 12 μL of 1.1 M dilute sulfuric acid. The concentrations of sulfuric acid and ammonium tetrathiomolybdate were $1.3x10^{-3}$ and $6.4x10^{-6}$ M with respect to the total microemulsion volume. The synthesis was done at a temperature of 50 °C. For the two-microemulsions synthesis method (Figure 1c), 5 mL of the two microemulsion systems, each containing 2.6 $x10^{-3}$ M sulfuric acid and $1.28x10^{-5}$ M ammonium tetrathiomolybdate, were mixed at 50 °C while bubbling nitrogen gas. Before mixing the microemulsion solutions, they were brought to a temperature of 50 °C while bubbling high purity nitrogen gas. In making ammonium tetrathiomolybdate impregnating solution, sodium hydroxide was added to enhance its dissolution in water. The concentration of sodium hydroxide with respect to 100 mL of $5x10^{-3}$ M thiomolybdate solution was $1x10^{-3}$ M.

Results and Discussion

Phase Behavior. The solubilization diagram of the microemulsion system 0.15 M NP-5/cyclohexane/water is shown in Figure 2a. The region between the solubilization (cloud point) and solubility (haze point) represents the one-phase microemulsion domain where the surfactant-stabilized microdroplets of water are dispersed in cyclohexane. The trend is consistent with the previously reported solubilization studies performed with polyoxyethylene nonylphenyl ether as the amphiphilic agent (Boakye et al., 1994; Osseo-Asare and Arriagada, 1990; Kon-no and Kitahara, 1970; Kitahara and Kon-no, 1966). For a non-ionic surfactant (e.g., NP-5), the solubility in the oil phase increases as the temperature is increased. This

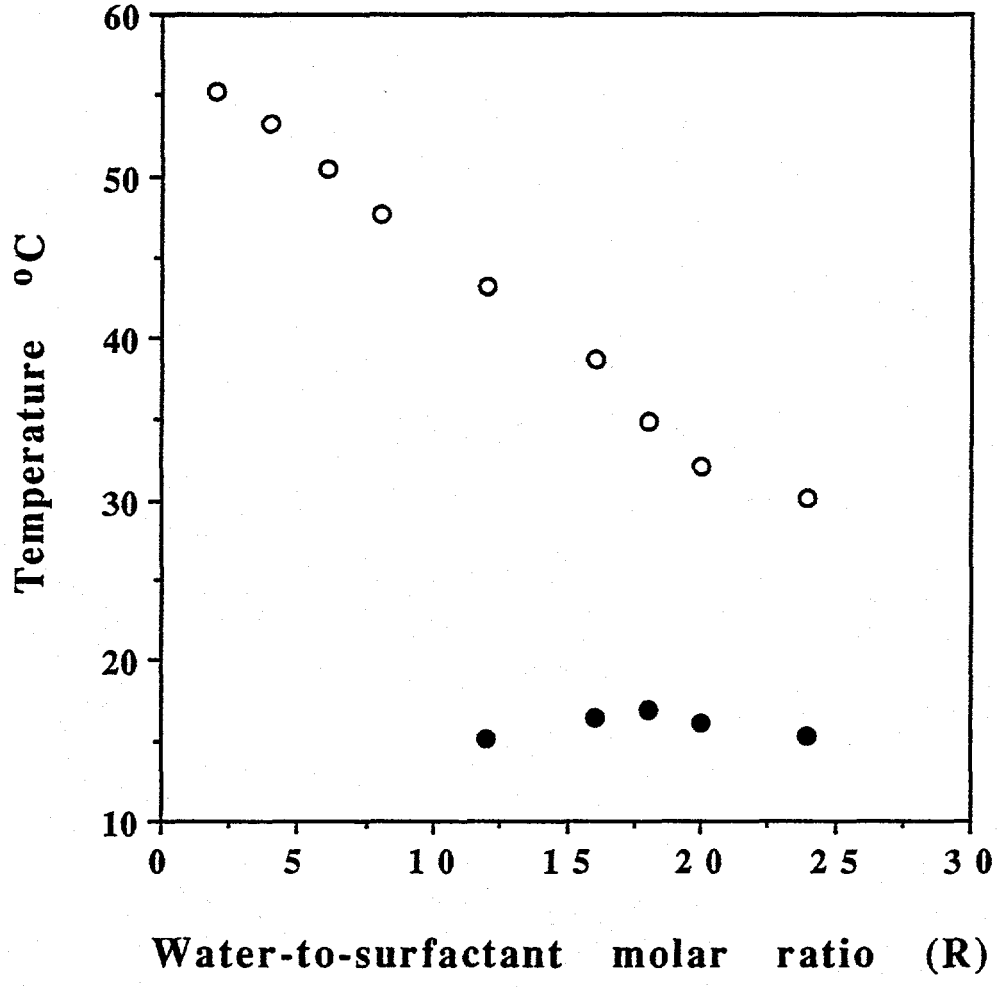

Figure 2a. Solubilization diagram of water in the microemulsion system 0.15 M NP-5/cyclohexane/water. ● , solubility limit; ○ , solubilization limit.

behavior is the result of decreasing strength of interaction between the etheroxy ethylene units and water molecules as the temperature is increased (Friberg et al., 1976). In other words, the hydrogen bond strength between the ether oxygen group and water is reduced, thus making the surfactant molecules more hydrophobic. Water-in-oil microemulsion coexists with excess water above the cloud point, whereas the surfactant phase containing dissolved water is separated from the oil below the haze point.

Figure 2b shows the effect of temperature on the solubility and solubilization limits for the NP-5/cyclohexane system with water and dilute sulfuric acid as solubilizates. The solubilization diagrams for water and acid are superimposed for easier comparison. No distinct differences are observed. Figure 2c summarizes the combined solubility and solubilization diagrams for the 0.15 M NP-5/cyclohexane system with water and ammonium tetrathiomolybdate as the aqueous domain. It is obvious that for the microemulsion system 0.15 M NP-5/cyclohexane/aqueous ammonium tetrathiomolybdate the one-phase microemulsion region is shifted downwards when compared to that of water as a solubilizate. Similar results were reported by Kon-no and Kitahara (1970) on the solubilization of acid, base and salt in the polyoxyethylene nonylphenyl ether/tetrachloroethylene system. They found that cations had no significant effect on the solubility diagram, but anions shifted the solubility and solubilization curves downwards. Furthermore, while the strong acid $HClO_4$ slightly elevated the solubilization curve, the relatively weak acids HCl and CH_3COOH hardly influenced the solubility and solubilization curves.

The differences in solubility curves obtained with ammonium tetrathiomolybdate and dilute sulfuric acid are discussed below using the following arguments: (a) the ether oxygen atom is a weak Lewis base and the water solubilized by the amphiphile is a weak Lewis acid; (b) the surfactant molecules are salted out by

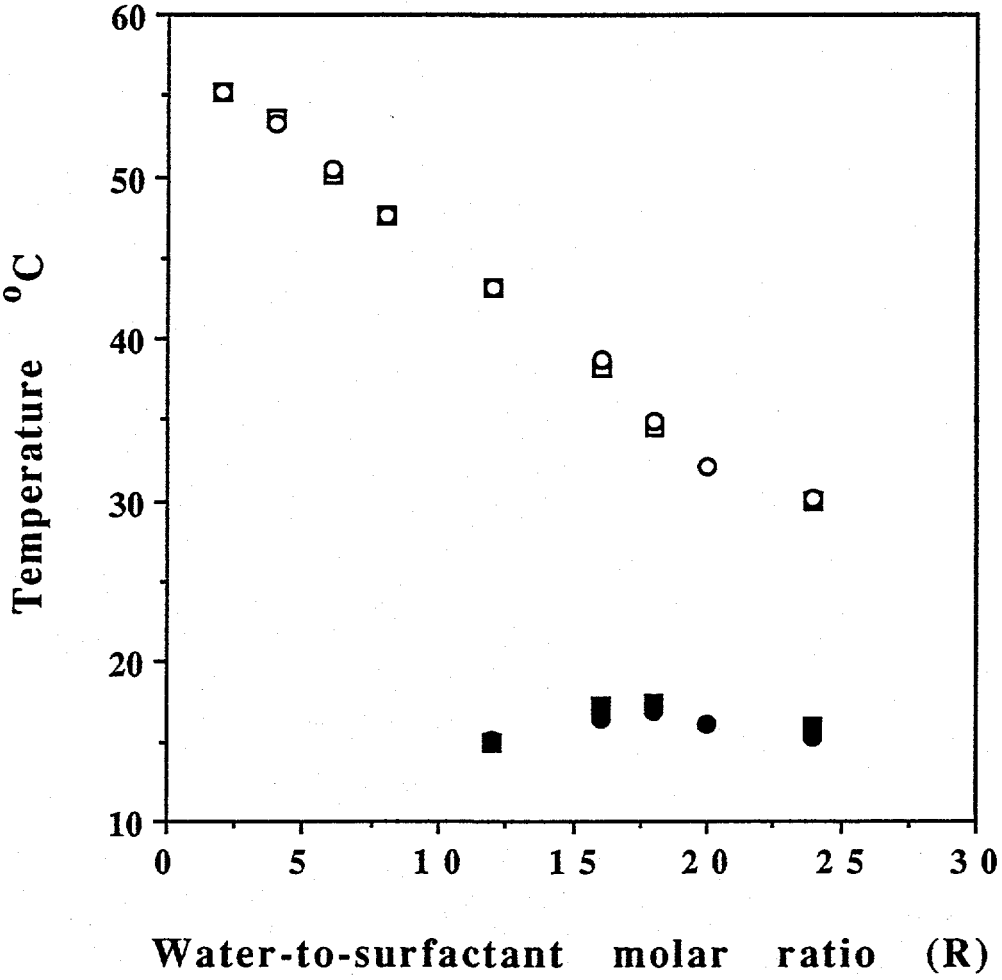

Figure 2b. Solubilization diagram of water and dilute sulfuric acid in the 0.15 M NP-5/cyclohexane/water microemulsion ([H_2SO_4] = 1.3×10^{-3} M).
● , solubility limit, H_2O; ○ , solubilization limit, H_2O;
■ , solubility limit, H_2SO_4; □ , solubilization limit, H_2SO_4.

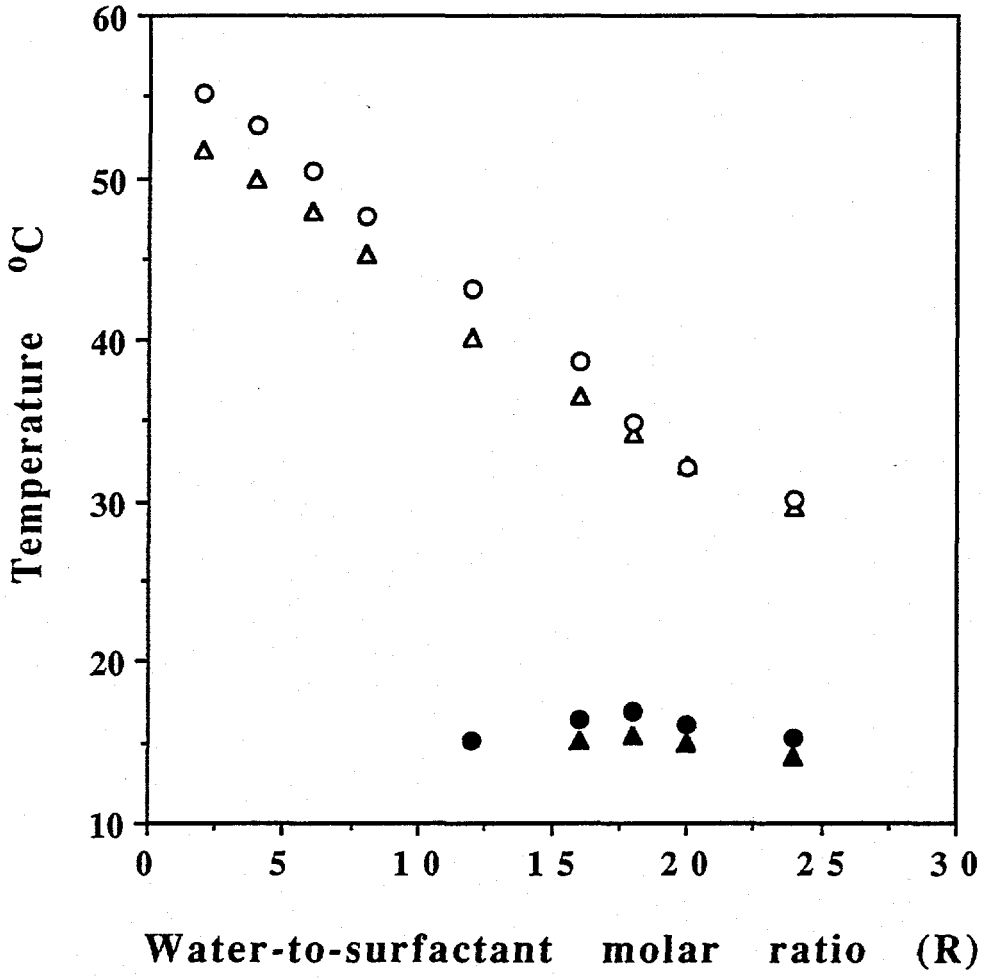

Figure 2c. Solubilization diagram of water and aqueous ammonium tetrathiomolybdate in the 0.15 M NP-5/cyclohexane/water microemulsion ($[MoS_4^{2-}] = 6.4 \times 10^{-6}$ M).

● , solubility limit, H_2O; ○ , solubilization limit, H_2O;

▲ , solubility limit, $(NH_4)_2MoS_4$; Δ , solubilization limit, $(NH_4)_2MoS_4$.

the presence of electrolytes. Also, in interpreting the solubilization data it should be borne in mind that the thiomolybdate solution contained $1x10^{-3}$ M sodium hydroxide.

Bases such as MoS_4^{2-} and OH^- will compete for water molecules with the oxygen atom of the oxyethylene group of the surfactant molecule. As a result, the extent of hydrogen bonding, which is the driving force for the solubilization of water in the microemulsion (Shich, 1962; Becher, 1962), is decreased. On the other hand, the addition of an acid will increase the extent of solubilization of water; since the acid is a proton donor, it will enhance the interaction between the water molecules and the ether oxygen. This interpretation is in support of the work done by Shich (1962) and Hsiao et al. (1956), who showed that the cloud point and the critical micelle concentration of nonionic surfactants in aqueous solutions increase as HCl is added, whereas they decrease by adding NaOH or salts. However, the elevation of the solubilization curve was not observed in this study.

Other investigators have offered an alternative explanation for this behavior, in terms of the 'salting out' mechanism (Mukherjee, 1965; Kizling and Stenius, 1987; Wiencek and Qutubuddin, 1991). This mechanism refers to the effective removal of water molecules from the ether oxygen group which is due to the preferential hydration of the solubilizates. In support of this view, Kon-no and Kitahara (1970) found that the cloud and haze points of the microemulsion system NP-8/tetrachloroethylene/water depended on the nature of the solubilized anion. The order of lowering in the solubilization diagram was $F^- > Cl^- > NO_3^- > I^- > SCN^-$. These results were rationalized using the argument that the more basic anion dehydrates the ether oxygen group to a greater extent, thus lowering the solubilization curve to a greater degree.

Effect of Electrolyte on Micellar Size. Presented in Figure 3 are the results of the micellar size measurements for the solvent system 0.15 M NP-5/cyclohexane with water, ammonium tetrathiomolybdate and aqueous sulfuric acid as solubilizates. For each solubilizate, the micellar diameter increases with the water-to-surfactant molar ratio (R). Furthermore, for each R value the microemulsion droplet size decreases on solubilizing ammonium tetrathiomolybdate or aqueous sulfuric acid.

Figure 4 summarizes the relationship between the surfactant aggregation number and R for each of the solvent systems. The micellar aggregation numbers were obtained from the hydrodynamic radii of the inverse micelles. For each microemulsion system the surfactant aggregation number first decreases with R to R~3 and then increases. The results for R<3 are unexpected since the decrease of aggregation numbers with increasing R suggests that the aggregation of the amphiphiles is favored at low R. The hydrodynamic diameters reported in Figure 3 are apparent values. At low water-to-surfactant molar ratio the micellar concentration is relatively high and hence the interaction between the inverse micelles needs to be considered (Kizling and Stenius, 1987). Also at high micellar concentration (low R) the probability of multiple scattering increases. The results at low R can therefore be corrected by remeasuring the diffusion coefficients of the inverse micelles at different degrees of dilution and calculating the true diffusion coefficient from Equation 2, followed by combination with the Stokes-Einstein equation to get the true micellar size.

$$D_{app} = D_{true}(1 + \alpha\phi) \qquad (2)$$

(The parameters α and ϕ are the interaction parameter and volume fraction of dispersed phase, respectively.) However, for the microemulsion system with water as the solubilizate, the results at R>3 do agree with the aggregation numbers for the same solvent system reported by Kitahara (1965) using light scattering methods.

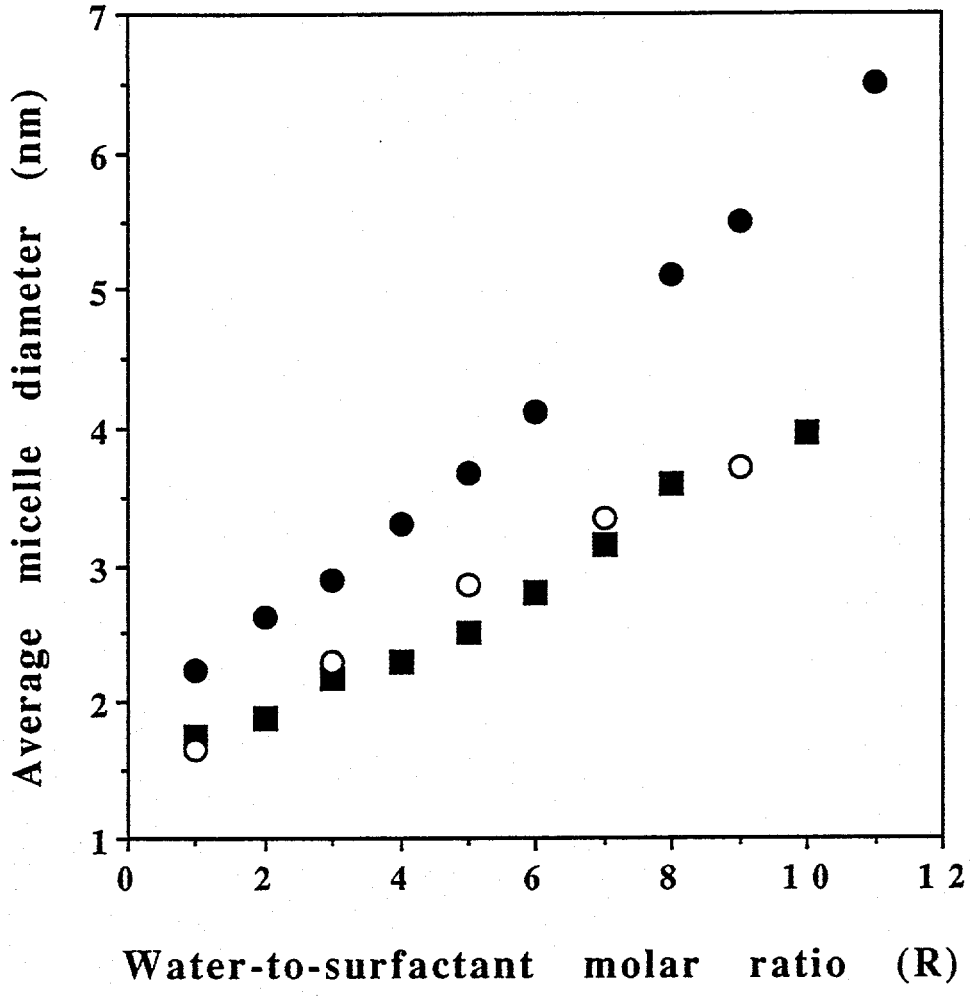

Figure 3. Photon correlation spectroscopic study of the variation of the hydrodynamic diameter with the water-to-surfactant molar ratio (R) for the microemulsion system 0.15 M NP-5/cyclohexane/water. ($[H_2SO_4] = 1.3 \times 10^{-3}$ M; $[MoS_4^{2-}] = 6.4 \times 10^{-6}$ M.) ●, water; ○, $[H_2SO_4] = 1.3 \times 10^{-3}$ M; ■, $[MoS_4^{2-}] = 6.4 \times 10^{-6}$ M.

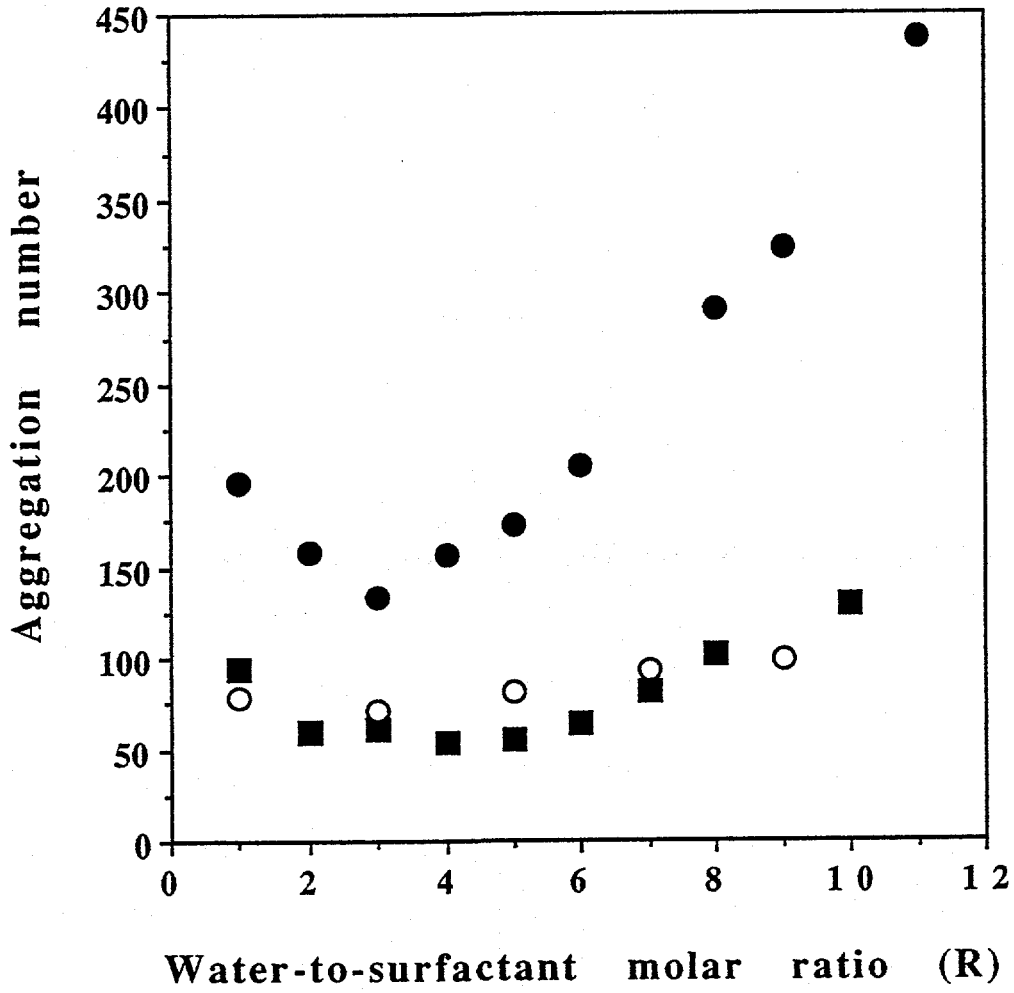

Figure 4. Effect of the water-to-surfactant molar ratio (R) on the micellar aggregation number for the microemulsion system 0.15 M NP-5/cyclohexane/water.
● , water; ○ , $[H_2SO_4] = 1.3 \times 10^{-3}$ M; ■ , $[MoS_4^{2-}] = 6.4 \times 10^{-6}$ M.

Furthermore, the aggregation numbers obtained at R<3 by extrapolating the values from R>3 are the same as those obtained by Kitahara and co-workers. Thus the aggregation numbers of the other microemulsions with aqueous sulfuric acid and ammonium tetrathiomolybdate were obtained by extrapolation in a similar manner.

For the same R value the decrease in micellar size when ammonium tetrathiomolybdate is substituted for water as solubilizate may be due to a combination of the following factors: (a) complexation through ion/dipole interaction between NH_4^+ and the poly(oxyethylene) chains (Chew et al., 1990) which reduces the effective concentration of surfactant molecules available for aggregation; (b) salting out of the surfactant molecules (i.e., dehydrating the ether oxygen), which increases the activity of the amphiphiles. This behavior can be correlated with low R values since the activity of the surfactants will be relatively high and the number of free water molecules available to promote aggregation is reduced.

The formation of oxonium ion in the ethylene oxide chains of nonionic surfactants makes them cationic in nature in aqueous solutions (Shich, 1962; Becher, 1962). This occurs if the water molecule attached to the ether oxygen of the amphiphile acquires a proton from the aqueous domain of the microemulsion fluid phase. The addition of secondary electrolytes decreases the effective size of the head group of the surfactant (double layer contraction). This causes the interface to be more rigid, reduces the intermicellar interaction, and hence reduces the aggregation number (Leung et al., 1988; Shinoda and Lindman, 1987; Chew et al., 1990). The formation of oxonium ion at the oxyethylene chains is more probable when an acid is a solubilizate. Thus the contribution of this effect (i.e., the cationic nature of the oxyethylene chain followed by secondary electrolyte addition) in reducing the micellar size is expected to be greater for dilute sulfuric acid as a solubilizate than for

ammonium tetrathiomolybdate. Furthermore, the ionic strength of the microemulsion with sulfuric acid as solubilizate is higher than that of the thiomolybdate species (e.g., 7.8×10^{-3} for the microemulsion with sulfuric acid as secondary electrolyte, and 2.1×10^{-5} for that with thiomolybdate ions). Therefore, for the same R value the surfactant aggregation number of the microemulsion system 0.15 M NP-5/cyclohexane/aqueous sulfuric acid is expected to be smaller than that of the microemulsion system with ammonium tetrathiomolybdate as the solubilizate. Contrary to expectation, this was not observed. Thus other factors (e.g., the nature of interaction of the oxyethylene chains with the solubilized species) may also be responsible for the decrease in the aggregation number. For the microemulsion system NP-5/cyclohexane/aqueous sulfuric acid, the presence of a proton donor in the micellar environment should encourage micellization and hence increase the aggregation number. This seems to be counteracted by the ionic strength effect as the presence of the acid decreased the aggregation number.

Particle Synthesis. Particles were synthesized in the microemulsion fluid phase utilizing the following synthesis protocols: (a) microemulsion-plus-a-second-reactant method as represented by Figures 1a and 1b; (b) two microemulsions (Figure 1c). Figure 5 is a summary of the results of the average particle diameter versus R for the various synthesis methods. Figures 6, 7 and 8 present the TEM micrographs of molybdenum sulfide particles synthesized using the three methods. Generally, for all the synthesis schemes the average particle diameter increases with R. Also within the limits of standard deviation of the average particle size, the diameter does not depend on the method of preparation for R values of 1-2.5. However, at $R>3$ the particle size (and the size distribution) depends on the synthesis method. The dependence of the particle size on the synthesis protocol is as follows: thiomolybdate-plus-acid solubilized in microemulsion $\approx$ two microemulsions $<$

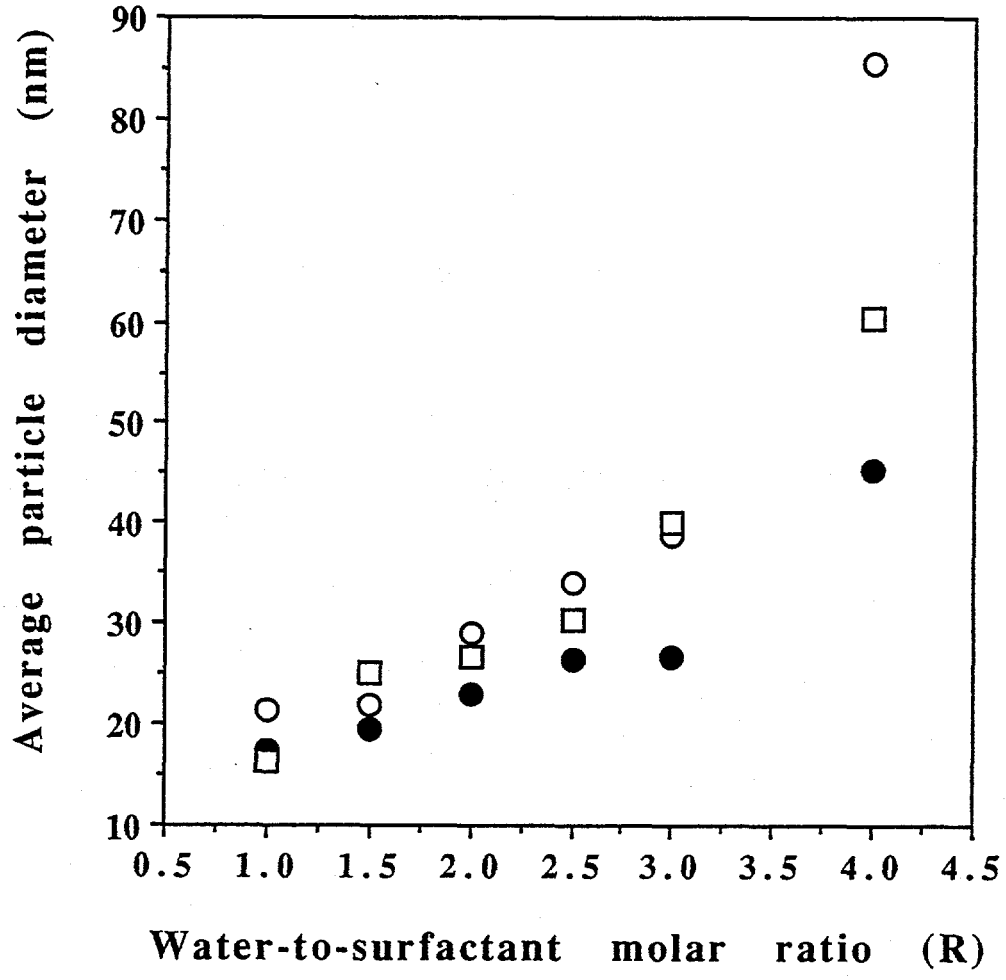

Figure 5. Effect of the water-to-surfactant molar ratio (R) on the average molybdenum sulfide particle size for the 0.15 M NP-5/cyclohexane/water microemulsion system using different synthesis protocols. ●, thiomolybdate-plus-acid solubilized in microemulsion (TPAM); ○, acid-plus-thiomolybdate solubilized in microemulsion (APTM); ❑, two microemulsions (TM).

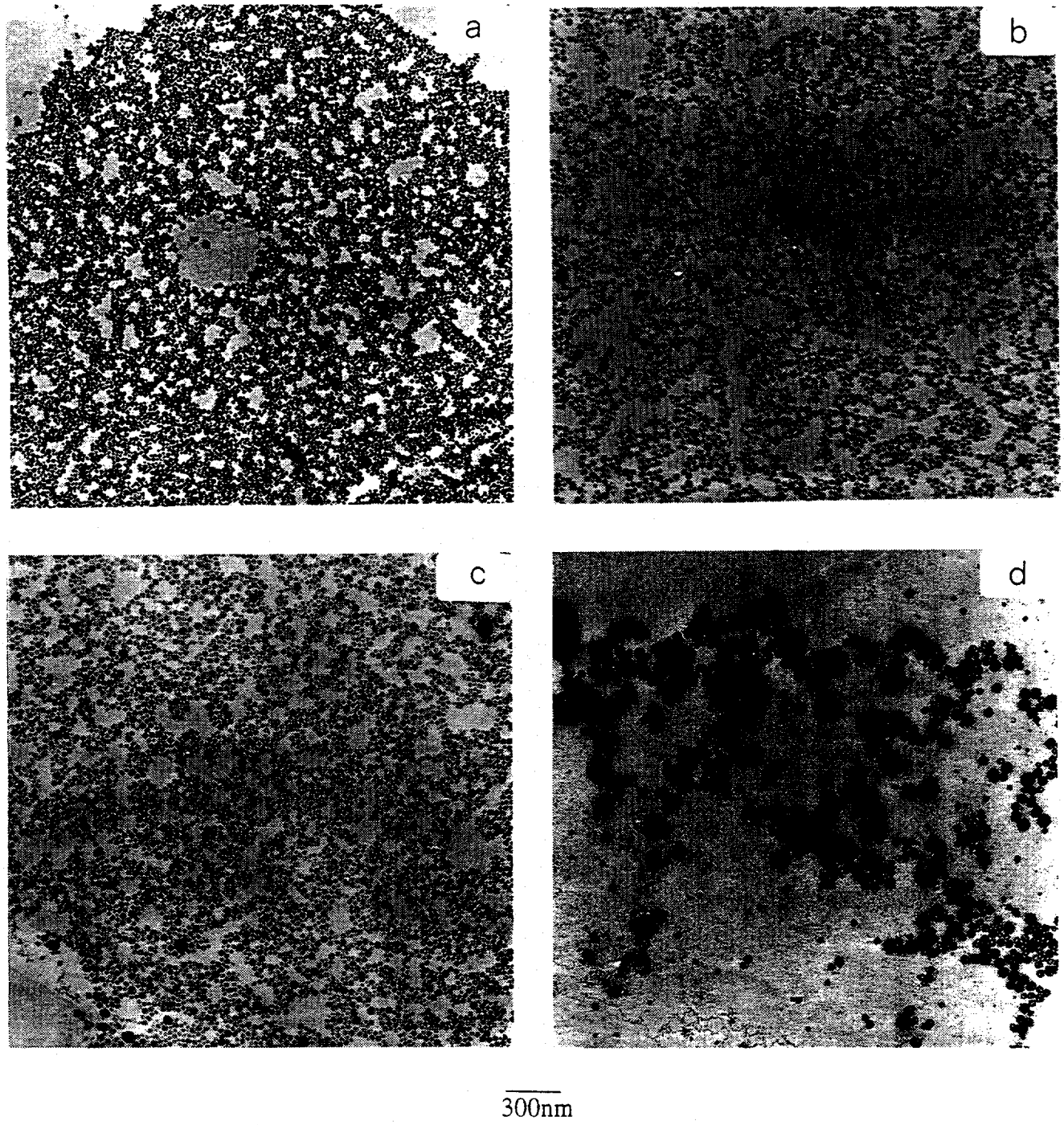

Figure 6. TEM micrographs of molybdenum sulfide particles prepared in the 0.15 M NP-5/cyclohexane/water microemulsion system. The thiomolybdate-plus-acid solubilized in microemulsion (TPAM) synthesis protocol was used. $[H_2SO_4] = 1.3 \times 10^{-3}$ M; $[MoS_4^{2-}] = 6.4 \times 10^{-6}$ M. (a) R=1; (b) R=2; (c) R=3; (d) R=4.

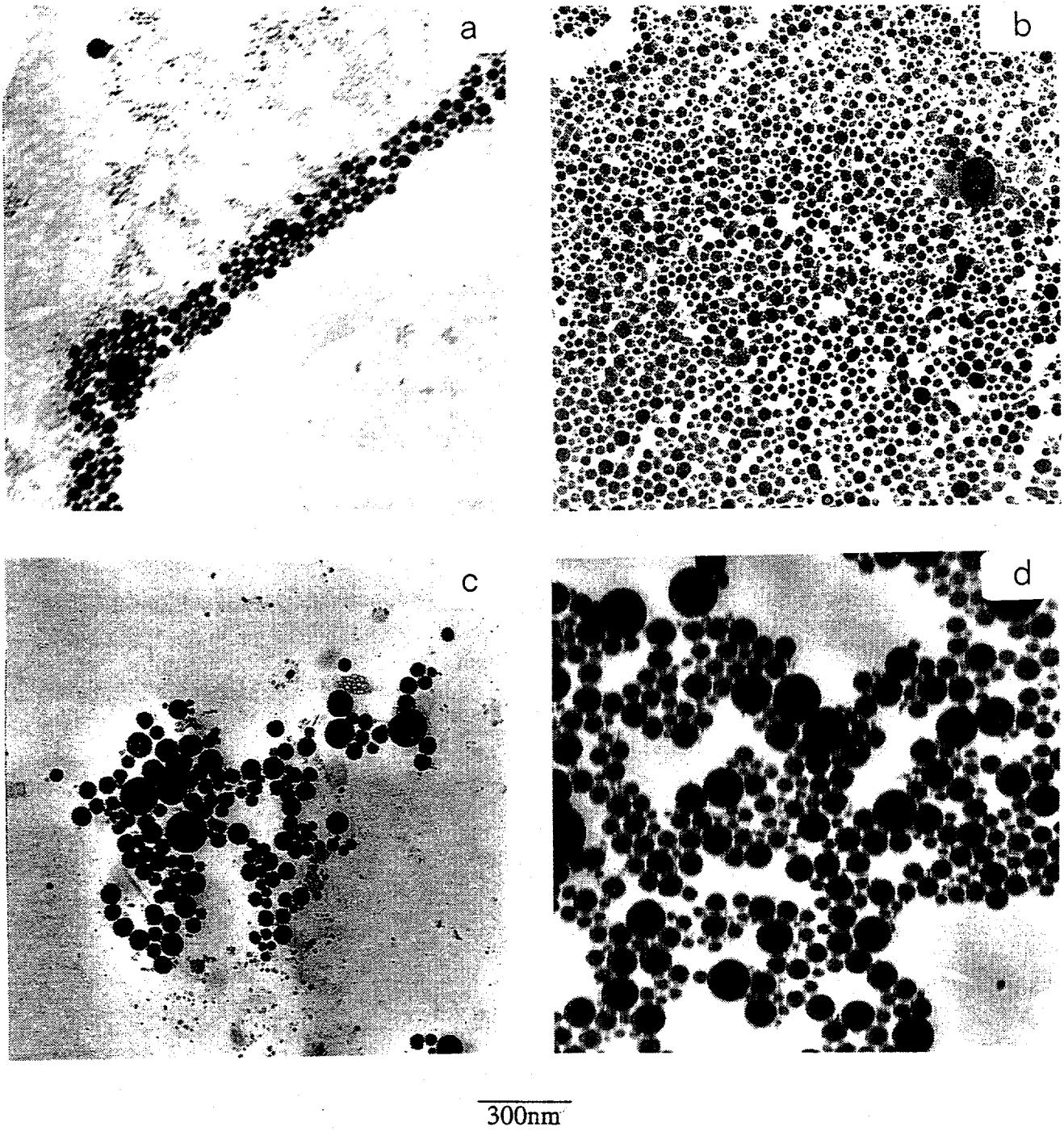

Figure 7. TEM micrographs of molybdenum sulfide particles prepared in the 0.15 M NP-5/cyclohexane/water microemulsion system. The two microemulsions (TM) synthesis protocol was used.
$[H_2SO_4] = 1.3 \times 10^{-3}$ M; $[MoS_4^{2-}] = 6.4 \times 10^{-6}$ M. (a) R=2; (b) R=2.5; (c) R=3; (d) R=4.

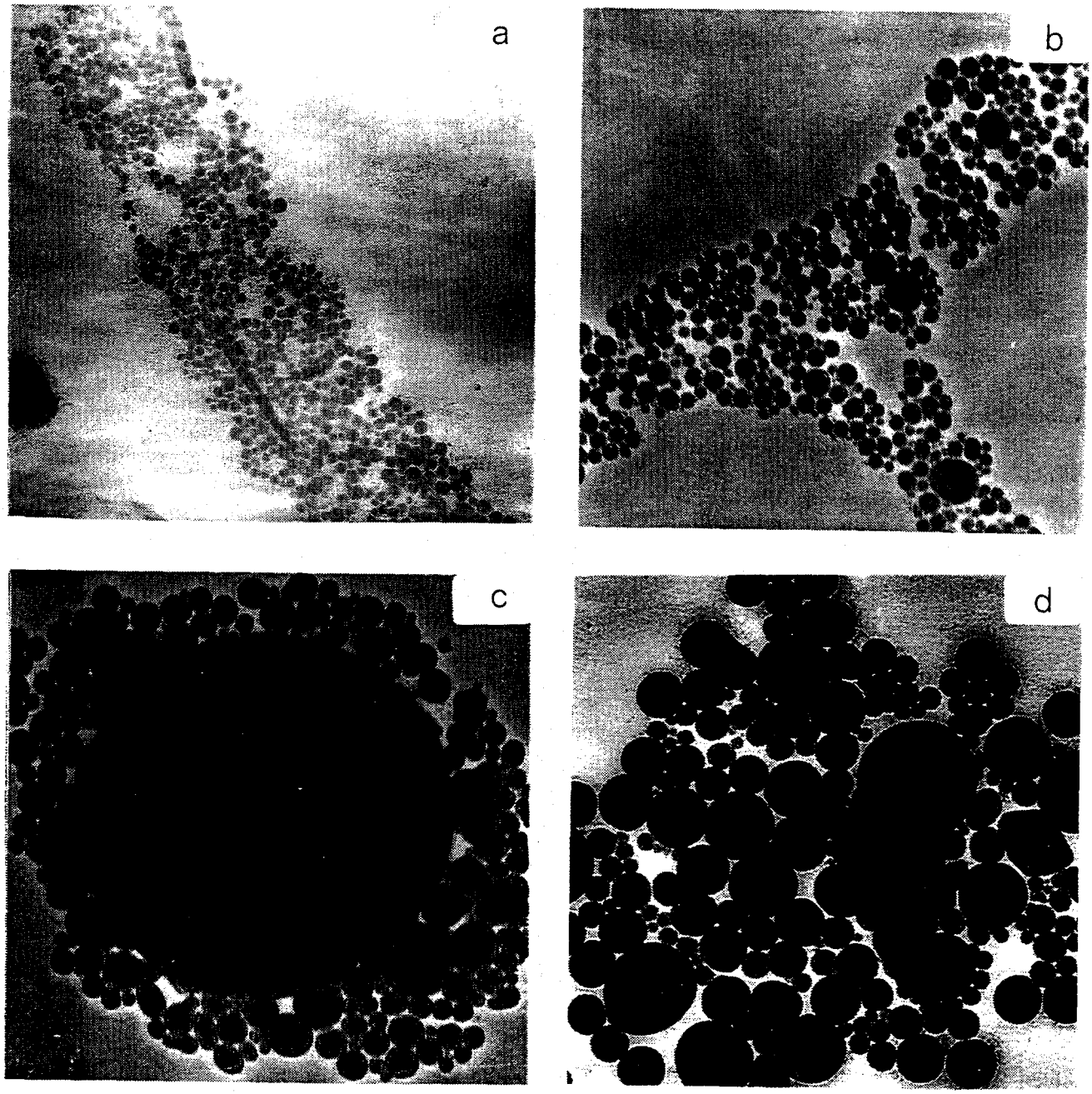

Figure 8. TEM micrographs of molybdenum sulfide particles prepared in the 0.15 M NP-5/cyclohexane/water microemulsion system. The acid-plus-thiomolybdate solubilized in microemulsion (APTM) synthesis protocol was used. $[H_2SO_4] = 1.3 \times 10^{-3}$ M; $[MoS_4^{2-}] = 6.4 \times 10^{-6}$ M. (a) R=2; (b) R=3; (c) R=3; (d) R=4.

acid-plus-thiomolybdate solubilized in microemulsion. At R=4 the particle size strongly depends on the synthesis protocol used and is in the order: thiomolybdate-plus-acid solubilized in microemulsion (TPAM) < two microemulsions (TM) < acid-plus-thiomolybdate solubilized in microemulsion (APTM).

To rationalize the results presented in Figure 5, the following particle formation scheme in w/o microemulsions is considered: (a) thiomolybdate and protons react in the water cores of the inverse micelles to form molybdenum sulfide monomers; (b) a critical number of molybdenum sulfide monomers combine in an inverse micelle to form a nucleus. The nuclei grow either by adding on monomers or by aggregating.

To reduce particle growth by aggregation, the rate of material transport between the microemulsion droplets must be controlled. The rate of fusion and fission of the inverse micelles is represented by the exchange constant (K_{ex}), which for the Triton X-100 microemulsion is ~10^8 (Almgren et al., 1986). The exchange constant increases when the water-to-surfactant molar ratio increases. Furthermore, as K_{ex} increases particle aggregation in the microemulsion fluid phase increases (Hou and Shah, 1988; Chew et al., 1990; Kandori et al., 1988).

Particle growth and polydispersity due to monomer addition can be controlled by increasing the rate of nucleation of the particles in the microemulsion. The nucleation rate in the microemulsion fluid phase is controlled by the parameter 'ion occupancy number' (Boakye et al., 1994; Nagy, 1989; Lianos and Thomas, 1988). It represents the number of reactant species in an inverse micelle. As the occupancy number is increased the supersaturation ratio increases and the nucleation rate increases. To obtain monodispersed particles, the nucleation and growth events should occur on different time scales. This means that a large number of nuclei is produced in a very short time followed by monomer addition. If the nucleation

period is long, new nuclei are formed while the old ones grow by monomer addition, which leads to polydispersity.

Presented in Tables 1 and 2 is a summary of data on the surfactant aggregation number (N), the number of inverse micelles (N_m), the average molybdate occupancy number (N_{oc}, i.e., the ratio of the number of tetrathiomolybdate ions to the number of inverse micelles), the number of particles in 10 mL of microemulsion (N_p) and the ratio N_m/N_p for various R values. The calculation of the average occupancy number was based on the assumption that the reactant species are confined to the cores of the inverse micelles. Furthermore, since the aggregation numbers were affected by the presence of the reactant species, the number of micelles was calculated using the measured diameter of the inverse micelle for the particular solubilized electrolyte.

From the N_{oc} data (Table 2), it is inferred that out of every 10^3 inverse micelles there is one thiomolybdate ion. This indicates that the formation of nuclei is limited by intermicellar exchange and that nucleation via intra-micellar interaction is negligible. Furthermore, N_{oc} increases according to the synthesis protocol: TPAM > TM > APTM. The implication of this trend for particle synthesis is that, as the molybdate occupancy number increases, the nucleation rate concomitantly increases (Nagy, 1989; Lianos and Thomas, 1988). Thus for a microemulsion with the same thiomolybdate concentration, the number of nuclei formed is expected to be in the order TPAM > TM > APTM. The number of excess monomers which were not utilized in nuclei formation will be in the order APTM > TM > TPAM. Therefore, by considering the monomer addition concept of growth, more monomers will add onto nuclei and primary particles when the synthesis protocol ATPM is used compared to TM and TPAM. Thus for each R value the particle size should increase according to the synthesis method: TPAM < TM < APTM. This is found to be true for R=4 and partially true for R=3 where the particle

Table 1

Statistical parameters for the formation of molybdenum sulfide particles prepared in the 0.15 M NP-5/cyclohexane/water microemulsion.

	TPAM			TM			APTM		
R	N	$N_m x10^{-19}$	$N_p x10^{-11}$	N	$N_m x10^{-19}$	$N_p x10^{-11}$	N	$N_m x10^{-19}$	$N_p x10^{-11}$
1	48	1.9	9.1	34	3.2	11.0	20	4.5	4.8
2	57	1.6	4.1	45	2.2	2.5	32	2.8	1.9
3	63	1.43	3.2	53	1.8	0.74	42	2.1	0.81
4	70	1.29	0.7	60	1.5	0.22	53	1.7	0.08

Table 2

Statistical parameters for the formation of molybdenum sulfide particles prepared in the 0.15 M NP-5/cyclohexane/water microemulsion.

	$N_{oc}x10^3$			$\frac{N_m}{N_p} x10^{-8}$		
R	TPAM	TM	APTM	TPAM	TM	APTM
1	2.1	1.2	0.85	0.21	0.29	0.94
2	2.4	1.7	1.4	0.38	0.87	1.45
3	2.7	2.2	1.8	0.45	2.4	2.6
4	3.0	2.6	2.3	1.8	6.9	22.4

diameter increases in the order TPAM ≈ TM < APTM. However, at R values of 1-2.5 the particle diameter is the same, within the limits of standard deviation of the average particle size. From Table 2 it is seen that, for each synthesis method, the occupancy number increases with R. This implies that the nucleation rate should increase with R and the particle size should decrease with R. However, contrary to expectation, the particle size increases with R. Hence the monomer addition concept of growth may not be operative here.

From Table 2 it is seen that the ratio N_m/N_p increases in the order TPAM < TM < APTM. It is also noted that for every 10^3 inverse micelles there is one thiomolybdate ion. As a first approximation we do assume that if two molybdenum sulfide monomers form a particle then the magnitude of the ratio N_m/N_p should be ~10^3. In contrast, out of every 10^8 inverse micelles only one particle forms. This suggests that particle aggregation occurs in the w/o microemulsion via micellar fusion. Furthermore, since aggregation of particles reduces the number of particles present in the microemulsion fluid phase, the ratio N_m/N_p should increase as R is increased. This is because the exchange of material between inverse micelles increases with the water-to-surfactant molar ratio. This is true for each synthesis method used.

It is interesting to note that both the ratio N_m/N_p and the extent of particle aggregation increase according to the synthesis protocol in the order TPAM < TM < APTM. This trend is in agreement with the mechanism of particle aggregation as outlined above and is further explained by referring to Figures 2a, 2b and 2c. It is seen that when thiomolybdate ion is used as solubilizate, the phase stability diagram is lowered by about 4 °C, especially at low R values, compared to the case when dilute sulfuric acid and water are used. At R=4 the solubilization limit is 50 ± 0.5 °C. Thus phase separation will be induced by first solubilizing ammonium thiomolybdate in the microemulsion at 50 °C. Observations made during

experiments showed some cloudiness. At this stage the solvent system 0.15 M NP-5/cyclohexane/thiomolybdate is composed of excess aqueous ammonium thiomolybdate and dispersed droplets of thiomolybdate and water in cyclohexane. The phase separation induces polydispersity since some particles are formed in the one-phase microemulsion system whereas others are not (e.g., Figures 7c, 7d, 8b, 8c and 8d). Furthermore, particles made outside the one-phase microemulsion domain will aggregate. An example is presented in Figure 8c where the TEM picture shows particles having an average size of 70 nm clustering around a central particle of 1200 nm. This behavior becomes less prominent as R is decreased, because the solubilization limit increases as R is decreased. This may be the reason why the extent of particle aggregation depends on the synthesis protocol at R=3 and R=4 while at R=1-2.5 there is no dependence. Furthermore, for the TM synthesis protocol, ammonium tetrathiomolybdate and acid are solubilized in separate microemulsions at 50 °C before mixing. Hence the microemulsion containing thiomolybdate ions will phase-separate at 50 °C but that containing acid will not. Thus it is reasonable to expect that particle aggregation will occur to a lesser extent when compared to the APTM method.

TASK 3: CATALYST TESTING

Experimental

Zeta Potential Measurements. Table 3 shows the proximate and ultimate analyses for the coals investigated. Slurries for the electrokinetic measurements were prepared by agitating 25 mg of coal with 250 mL of 10^{-2} M KNO_3 solution (indifferent electrolyte) in Nalgene bottles for 24 h. Zeta potential measurements

Table 3

Data for Coal Samples

Sample Designation	**PSOC-1401**	**DECS-6**
Seam	Canyon Top	Blind Canyon
State	Wyoming	Utah
Country	USA	USA
ASTM Rank	Subbituminous B	HVA bituminous
Moisture (as received, wt%)	16.33	4.73
Mineral Matter (dry, wt%)	5.72	5.84
Elemental Composition		
Carbon	72.70	81.87
Hydrogen	4.62	6.29
Nitrogen	1.07	1.56
Sulfur (organic)	0.28	0.40
Oxygen (by difference)	21.38	10.10

were made using an electrophoresis apparatus (Zeta-Meter, Inc.). Hydrochloric acid and ammonium hydroxide were used to control the pH in the acidic and basic regions. All the experiments were conducted at room temperature (25 ± 4 °C).

Coal Impregnation with Catalyst. The coal was first crushed to pass a 60 mesh sieve. Impregnation with ammonium heptamolybdate (1% Mo (daf), expressed as elemental Mo) was accomplished as follows: the Mo salt was dissolved in sufficient distilled water in a flat-bottom flask to give an approximate water-to-coal ratio of 1:1 (v/v), and coal was added to this solution. Three samples were prepared in this fashion, the slurry pH being adjusted in two cases using either conc. HCl or conc. NH_4OH. After stirring for 30 min, the slurry pH was measured and the coal was dried in vacuum (for 2 h at 100 °C), removed and stored in tightly stoppered glass vials until further use.

Liquefaction Tests. These were conducted in 25 cc microautoclave reactors (tubing bombs) in a preheated fluidized sand bath. For each reaction, 1.5 g of coal, 1.5 g of tetralin, and 25 mg of CS_2 (approx. 2.2 times the amount of sulfur required to convert all the Mo to MoS_2) were charged into the reactor. Air was removed by repeatedly pressurizing the reactor to 6.9 MPa, once with nitrogen and twice with hydrogen. Subsequently, the reactor was pressurized to 6.9 MPa (cold) with hydrogen. It was then plunged into the sandbath and agitated at 200 cycles per minute. Reaction temperature and residence time were 350 °C and 30 min, respectively. At the end of this time, the reactor was plunged into cold water to quench the reaction. After depressurizing the reactor, its contents were rinsed with hexane into a dried soxhlet thimble and extracted overnight under nitrogen. The hexane was removed from the extract by rotary evaporation. The hexane-insoluble residue was then soxhlet-extracted with THF to separate asphaltenes from the

residue. The THF was removed from the extract by rotary evaporation. Asphaltenes and residue were dried for 6 h and 2 h, respectively, in vacuum at 100 °C. Conversion was calculated by subtracting the weight of the residue from the weight of the coal and dividing by the daf weight of the coal.

Results

Testing of Microemulsion-Based Catalyst. In our previous reports, we described liquefaction results obtained with the bituminous coal chosen for this study (DECS-6). Briefly, it was found that, while testing in the *in situ* mode, both the cosurfactant (benzyl alcohol) and the surfactant (NP-5) used in formulating the microemulsion introduced undesirable solvent effects into the process. In order to verify and further explore these effects, an analogous set of experiments was performed using the subbituminous coal selected for this investigation (PSOC 1401).

Table 4a shows the results obtained with the subbituminous coal. Comparing Runs 74 and 76, it can be seen that the effect of adding tetralin is to accelerate the dissolution of coal, with no observed change in the oil yield. This is consistent with the conventional view that hydrogen donor (or catalyst) - when present - functions mainly to provide hydrogen for capping generated radicals. When benzyl alcohol is used as the solvent (Run 77), the yield of oils becomes negative. Since the latter is calculated by difference, this result suggests that benzyl alcohol - initially hexane-soluble - has been transformed into hexane-insoluble material. The high "yield" of asphaltenes is an artifact of this transformation. That is, benzyl alcohol (and not coal) has been transformed into (hexane-insoluble, THF-soluble) asphaltenes. This finding is also consistent with a recent report in the literature (Saini et al., 1993). Run 62 indicates that the surfactant (NP-5) also transforms into hexane-insoluble material under these conditions, albeit to a lesser extent.

Table 4a

Summary of Data for Thermal Runs with Subbituminous Coal

Test No.	Solvent[a]	Solvent-to-Coal Ratio	Conversion (% daf)		
			Total[b]	Asphaltenes[c]	Oils[d]
LT 74	None	-	12.3	12.3	0.0
LT 76	Tetralin	2.0	24.5	24.5	0.0
LT 77	BA[e]	2.0	18.6	45.2	-26.6
LT 62	Surfactant[f]	1.3	13.3	17.8	-4.5
LT 20	BME[g]	5.6	28.6	ND	ND

Table 4b

Summary of Data for Catalyzed Runs with Subbituminous Coal

Test No.	Catalyst loading (ppm)	Solvent[a]	Solvent-to-Coal Ratio	Conversion (% daf)		
				Total[b]	Asphaltenes[c]	Oils[d]
LT 75	10,000	None	-	29.2	23.4	5.8
LT 7	10,000	Tetralin	2.5	24.9	6.1	18.8
LT 17	50	MLME[h]	5.6	37.4	ND	ND

[a] Liquid vehicle.

[b] Based on THF-insoluble residue.

[c] THF-soluble, hexane-insoluble fraction.

[d] Hexane-soluble fraction.

[e] Benzyl alcohol.

[f] Surfactant = NP-5.

[g] Blank microemulsion (0.4 M NP-5/tetralin/benzyl alcohol/water).

[h] Metal-loaded microemulsion (0.4 M NP-5/tetralin/benzyl alcohol/water).

Run 20 does not lend itself to straightforward interpretation. The total conversion suggests that the benzyl- alcohol-based microemulsion is in fact a good liquefaction medium, even when compared to tetralin (Run 76). However, several additional factors must be considered. First, the amount of "solvent" in relation to coal is very high. The higher conversion obtained may be the result of more efficient dispersion of coal fragments during reaction. Second, it was impossible to recover all the products from the reactor (despite repeated rinsing with THF and scraping with a spatula) since they were extremely gummy and tarry and stuck fast to the reactor walls. (Obviously, failure to recover a portion of the insoluble residue will register as an increase in the total conversion.) Third, it was not possible to perform product work-up as before, because the products were viscous and tar-like and it was extremely difficult to separate the asphaltenes from the hexane-solubles.

Table 4b shows the results obtained with catalyst present. From Run 7 it is seen that the presence of tetralin contributes to a three-fold increase in the oils yield relative to the dry (solvent-free) case (Run 75). Again, the results with the metal-loaded microemulsion were disappointing. The products were very difficult to remove completely from the reactor and impossible to fractionate. The conversions reported in the table are misleading and no doubt due to one or more of the experimental factors listed above in the discussion of Table 4a.

We conclude, therefore, that the microemulsion medium used here is an extremely poor coal liquefaction medium. The lack of a catalytic effect of a metal-loaded microemulsion is attributed to the complete masking of the catalytic activity by the solvent-induced retrogressive reactions.

Role of Coal Surface Chemistry in Impregnation with Catalyst. The objective of this part of the work was to study the surface chemistry of coal with a view to better understand the factors that influence the uptake of catalyst precursor from aqueous solution. This may have important implications for achieving high dispersions

(Solar et al., 1991; Abotsi et al., 1992). A total of four samples were studied - two coals, as-received (whole) and demineralized.

The surface charge was monitored as a function of pH as described above. Figure 9 shows the results obtained with the subbituminous coal. The as-received coal is negatively charged over the entire range of pH studied. Similar results with another subbituminous coal (PSOC 1485) have been reported (Abotsi et al., 1992). Demineralization has two effects: (a) it reduces the total negative charge on the coal at pH>4, and (b) it renders the coal positively charged at pH<4. This seems to indicate that mineral matter plays a significant role in determining the charge on a coal surface (Siffert and Hamieh, 1989; Hamieh and Siffert, 1991).

The next step was to study the implications of the above observations for coal liquefaction. Briefly, if the coal surface can be rendered less negative (or even positive) by adjusting solution pH to be highly acidic, then interaction between molybdenum anions and coal should be favored. This in turn would permit a more efficient use of any catalyst anchoring sites on the coal surface.

To test this hypothesis, three coal samples were prepared, each impregnated with ammonium heptamolybate at a different pH. (The details of the loading procedure are given in the experimental section.) Table 5 shows the conversion data. It is seen that when the pH is rendered highly acidic (Run 77, pH=1.1) using HCl, the oils+gas yield *decreases* drastically by about a factor of four relative to the unadjusted case (Run 78, pH=5.0). In rationalizing this, the work of Dun et al. (1985) and Solar et al. (1991) is helpful. Both groups found no major differences in the catalytic activity of Mo/C catalysts with varying pH. Solar et al. invoked the adsorption model of Cruywagen and de Wet (10) to explain this observation. According to them, polymerization of molybdenum oxyanions at low pH is responsible; polymeric Mo species may not adsorb strongly on the support, and thus

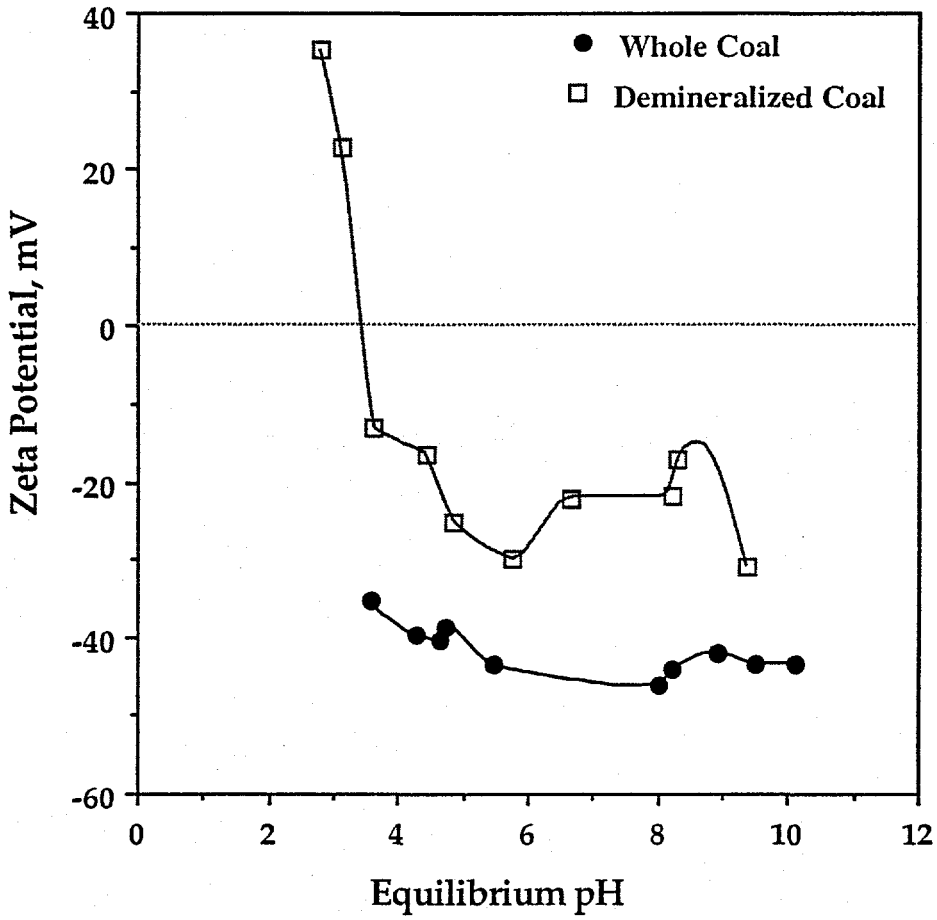

Figure 9. Zeta potential vs. equilibrium pH for the subbituminous coal.

Table 5

Conversion Data for Subbituminous Coal Impregnated at Different pHs

Test No.	Final pH of slurry	Conversion (% daf)		
		Total[a]	Asphaltenes[b]	Oils[c]
LT 77	1.1	41.8	36.7	5.1
LT 78	5.0	38.3	16.5	21.8
LT 79	10.1	24.2	11.5	12.7

[a] Based on THF-insoluble residue.

[b] THF-soluble, hexane-insoluble fraction.

[c] Hexane-soluble fraction.

be more prone to sintering upon catalyst activation. Furthermore, the formation of polymeric species adversely affects the impregnation process itself. It is believed that $Mo_8O_{26}^{4-}$ predominates at pH<2.

Comparing Runs 78 and 79, it is seen that the adjustment of the pH to 10.1 has an adverse effect on yields of both asphaltenes and oils+gas. This is being analyzed further.

CONCLUSIONS

Solubilization of the secondary electrolytes in the solvent system 0.15 M NP-5/cyclohexane shows that the one-phase microemulsion domain depends on the solubilizate. Dilute sulfuric acid did not have any apparent effect on the solubilization diagram, but the solution of thiomolybdate and hydroxide ions shifted the solubility domain downwards. The sizes of the inverse micelles were found to depend on the nature of the secondary solubilizate. The micellar aggregation number decreased when dilute sulfuric acid and the thiomolybdate ions were solubilized. At R=3 and R=4 the average particle size was found to depend on the synthesis protocol. No dependence was found at R=1-2.5.

The possible catalytic effects of highly dispersed MoS_2 particles (synthesized as described above) in the liquefaction of both a bituminous and a subbituminous coal are masked by retrogressive reactions which are promoted by the components of the microemulsion.

REFERENCES

Abotsi, G. M. K., K. B. Bota and G. Saha, *Energy Fuels* **6**, 779 (1992).

Almgren, M., J. van Stam, S. Swarup and J. E. Löfroth, *Langmuir* **2**, 432 (1986).

Becher, P., *J. Coll. Sci.* **17**, 325 (1962).

Boakye, E., L. R. Radovic and K. Osseo-Asare, *J. Coll. Interf. Sci.*, in press (1994).

Chew, C. H., L. M. Gan and D. O. Shah, *J. Dispers. Sci. Technol.* **11**, 593 (1990).

Cruywagen, J. J. and H. F. de Wet, *Polyhedron* **7**, 547 (1988).

Dun, J. W., E. Gulary and K. Y. S. Ng, *Appl. Catal.* **15**, 247 (1985).

Friberg, S. E., I. Lapczynska and G. Gillberg, *J. Coll. Interf. Sci.* **56**, 19 (1976).

Hou, M. J. and D. O. Shah, in" Interfacial Phenomena in Biotechnology and Materials Processing" (Y. A. Attia, B. M. Moudgil and S. Chander, Eds.), Elsevier, 1988, p. 443.

Hsiao, L., H. N. Dunning and P. B. Lorenz, *J. Phys Chem.* **60**, 657 (1956).

Kandori, K., K. Kon-no and A. Kitahara, *J. Coll. Interf. Sci.* **122**, 78 (1988).

Kitahara, A. and K. Kon-no, *J. Phys. Chem.* **70**, 3394 (1966).

Kitahara, A., *J. Phys. Chem.* **69**, 2788 (1965).

Kizling, J. and P. Stenius *J. Coll. Interf. Sci.* **118**, 482 (1987).

Kon-no, K. and A. Kitahara, *J. Coll. Interf. Sci.* **34**, 221 (1970).

Leung, L., M. J. Hou and D. O. Shah, in "Surfactants in Chemical/Process Engineering" (D. T. Wasan, M. E. Ginn and D. O. Shah, Eds.), Surfactant Science Series, Vol. 28, Marcel Dekker, New York, 1988.

Lianos, P. and J. K. Thomas *J. Coll. Interf. Sci.* **117**, 505 (1987).

Lianos, P. and J. K. Thomas, in " Materials Science Forum", Vol. 25-26 (G.E. Murch and F. H. Wohlbier, Eds.), 1988, p. 369.

Mukherjee, P., *J. Phys. Chem.* **69**, 4038 (1965).

Nagy, J. B., *Coll. Surf.* **35**, 201 (1989).

Osseo-Asare, K. and F. J. Arriagada, *Coll. Surf.* **50**, 321 (1990).

Saini, A. K., M. M. Coleman, C. Song and H. H. Schobert, *Energy Fuels* **7**, 328 (1993).

Shinoda, K. and B. Lindman, *Langmuir* **3**, 135 (1987).

Siffert, B. and T. Hamieh, *Coll. Surf.* **35**, 27 (1989).

Hamieh, T. and B. Siffert, *Coll.Surf.* **61**, 83 (1991).

Shich, M. J., *J. Coll. Sci.* **17**, 801 (1962).

Solar, J. M., F. J. Derbyshire, V. H. J. de Beer and L. R. Radovic, *J. Catal.* **129**, 330 (1991).

Wiencek, J. M. and S. Qutubuddin, *Coll. Surf.* **54**, 1 (1991).